Journal Home Page: https://sjes.univsul.edu.iq/

Research Article: Multi-Dam Failure Propagation in a Transboundary River System: A Case Study of Azad–Daryan–Hirwa–Darbandikhan Cascade

Fryad Hama Ibrahim[1,a,*]
Kawa Zaidan Abdulrahman[2,a]
[a] Department of Water Resources Engineering, College of Engineering, University of Sulaimani

Article Information

Article History:
Received: August 25th, 2025
Accepted :October 12, 2025
Available online: December, 2025

Keywords:
HEC-RAS, Dam Failure, Dam Stability, Inundation Map, Flood Hazard Map.

About the Authors:
Corresponding author:
Fryad Hama Ibrahim
E-mail: Fryad.ibrahim@univsul.edu.iq
Researcher Involved:
Kawa Zaidan Abdulrahman
kawa.abed@univsul.edu.iq

DOI https://doi.org/10.17656/ sjes.102000

Abstract

This study investigates the hydrodynamic consequences of cascading dam failures within a transboundary reservoir network involving the Azad, Daryan, and Hirwa dams in western Iran, and their downstream impact on the Darbandikhan Dam in northeastern Iraq. Using HEC-RAS 6.6 2D modeling, four breach scenarios were developed, with two key cases sequential overtopping and mixed-mode failure analyzed in detail. Simulations revealed that Scenario 1, involving full-capacity overtopping, poses the highest risk, with flood waves propagating rapidly through narrow valleys and causing peak water surface elevations of 512.0 m at the Iran–Iraq border and 491.55 m near Darbandikhan Dam, overtopping the spillway gates set at 485.0 m. Over 1,000 houses between Azad, Daryan and Hirwa dams are projected to be submerged, and Hirwa Village is completely inundated under flood depths exceeding 22 meters. Downstream in Iraq, at least 12 villages inundated under flood depths exceeding 2.5m and more than 70 km² of agricultural land are affected, including major infrastructure such as the Halabja highway, submerged under over 2m of floodwater. Flow velocities ranging from (10 to 25 m/s) exceed sediment entrainment thresholds, indicating substantial erosion, sediment transport, and long-term morphological impacts on reservoir banks and channels. The findings underscore the urgent need for structural improvements, dynamic reservoir operation protocols, real-time monitoring, and cross-border emergency coordination. The study also highlights the importance of incorporating geomorphic and climatic factors into future dam safety strategies.

1 Introduction

Dams serve a broad range of purposes, including flood control, potable water supply, agricultural irrigation, industrial support, and hydroelectric power generation **[1]**. However, without rigorous site-specific design, geotechnical evaluation, and hydrological assessment, the risks posed by dam infrastructure can become catastrophic. Dam failures, although relatively rare, release enormous volumes of water at high velocities, which can result in extensive damage to downstream environments, infrastructure, and human settlements. Given the potentially devastating consequences of dam breaches particularly in populated regions, assessing dam failure mechanisms and modeling associated flood risks are of paramount importance. These evaluations typically include breach formation dynamics, routing of flood hydrographs, and delineation of inundation zones. Despite their critical importance, comprehensive studies on cascade dam failure scenarios remain underrepresented in global literature. Flood waves generated by structural collapse can travel rapidly downstream, posing immediate threats to both life and property. Between 2000 and 2019, more than 450 major dam failures were recorded worldwide, resulting in substantial loss of life and economic damage **[2]**. Dam failures arise from multiple causes, including overtopping, piping, foundation instability, landslides, seismic shocks, and in rare cases, sabotage **[3,4]**. Among these, overtopping and internal erosion (piping) are the

leading failure modes **[1,5,6]**. Historical records show that overtopping accounts for approximately 38% of global dam failures, typically due to undersized spillways, while another 33% are attributed to seepage-induced piping **[7]**. The severe consequences of such events have necessitated the development of robust analytical frameworks and simulation models to predict flood impacts, inform emergency planning, and mitigate downstream hazards **[8-11]**.Numerous computational tools have been developed to simulate dam breach dynamics and downstream inundation. Prominent models include DAMBRK **[12]**. MIKE, and the HEC-RAS platform developed by the U.S. Army Corps of Engineers **[13]**. The DB-IWRH model, a physically based dam breach simulation framework developed by the Chinese Institute of Water Resources and Hydropower Research, is another widely applied tool in this domain **[14]**. Among these, HEC-RAS has become the most extensively used due to its two-dimensional capabilities, integration with GIS, and ease of coupling with terrain and hydrologic data. Numerous studies have successfully employed HEC-RAS to simulate dam failures and analyze their consequences **[15-21]**. The Iran–Iraq border, encompassing the Diyala River basin, is a seismically active zone that includes several major dams such as Azad, Daryan (Iran) and Darbandikhan (Iraq). The Mw 7.3 earthquake that struck the region on November 12, 2017, caused observable structural damage to the Darbandikhan Dam, underscoring its seismic vulnerability and the cascading risk posed by failures at upstream structures **[22]**.In response, dam authorities have adopted a more conservative operational approach, maintaining the Darbandikhan reservoir below its rule curve to accommodate potential inflow surges from upstream breaches. In this context, the present study investigates the transboundary hydrodynamic consequences of potential sequential failures of the Azad, Daryan, and Hirwa dams on the stability and operational integrity of the downstream Darbandikhan Dam. Using HEC-RAS version 6.6, a two-dimensional modeling approach is employed to simulate the flood wave propagation, peak discharge dynamics, and inundation patterns across multiple breach scenarios. The study has two primary objectives: (1) to assess the structural and hydrodynamic response of the Darbandikhan Dam under compound flood wave loads; and (2) to identify vulnerability thresholds that can inform adaptive reservoir management strategies and enhance regional Emergency Action Plans (EAPs).

2 Materials and Methods

2.1 Study Area

As shown in Fig. (1) is conducted within the transboundary Diyala River basin, which spans portions of western Iran and northeastern Iraq and hosts a complex system of interconnected reservoirs and dams. Four major hydraulic structures Azad, Daryan, Hirwa, and Darbandikhan are the focal points of this research due to their critical roles in regional water supply, hydropower generation, and flood regulation. Darbandikhan Dam Fig. (2), located approximately 65 km southeast of Sulaimani City and 230 km northeast of Baghdad, represents a key multipurpose infrastructure in Iraq. It is a rockfill embankment dam with a structural height of 128 m, a crest length of 445 m, and a full reservoir level at 485 m elevation. Designed for hydroelectric power production, irrigation, and flood control, the dam operates with three Francis turbines and possesses a storage capacity of 2.55 billion cubic meters. Due to its location upstream of populated centers such as Kalar and Diyala, and its substantial storage volume, Darbandikhan is classified as a high-risk asset in the event of upstream hydraulic failure. Upstream in Iran, the Azad Dam shown in (Figure 3) is situated on the Gura River approximately 40 km west of Sanandaj in Kurdistan Province. This embankment dam, located at coordinates (35°20'08.6"N and 46°32'58.5"E), stores up to 300 million cubic meters of water and supports agricultural, industrial, and municipal demands in the Qorveh–Dehgolan Plains while also generating 10 MW of hydropower **[23]**. Further downstream, the Daryan Dam shown in (Figure 4), constructed on the Sirwan River in Paveh County, Kermanshah Province, lies about 56 km upstream of Darbandikhan. Operational since 2015, this rockfill dam stands 169 m high and impounds a reservoir with a capacity of 316.3 million cubic meters **[24]**.

Adjacent to Daryan is the Hirwa Dam as shown in (Figure 5), a concrete diversion structure located roughly 8 km downstream, built in 2018 in Hirwa Village. Although relatively small with a height of 45 meters and a storage volume of 12 million cubic meters Hirwa plays an essential role in regulating flows before their diversion through the Nowsud Tunnel system **[25]**.

2.2 Problem Statement

The Diyala River basin as shown in (Figure 6), straddling the border between Iran and Iraq, is characterized by both seismic activity and hydrological complexity. Within this setting, the Darbandikhan Dam is currently operated below its standard rule curve as a precautionary measure. This conservative management strategy provides additional flood buffering capacity to account for unanticipated inflow surges that may arise from upstream dam failures, particularly under the compounded stress of seismic events and evolving climate patterns. This study employs HEC-RAS 2D hydraulic modeling to simulate hypothetical breach scenarios at Azad, Daryan and Hirwa Dams and to evaluate their downstream impact on the operational stability of Darbandikhan Dam. As a key multipurpose asset in the region, Darbandikhan Dam plays a vital role in electricity generation, irrigation, flood control, and water supply. However, the structure faces growing vulnerability due to two converging challenges: diminished inflow volumes caused by upstream

reservoir developments in Iran **[26]**, and the intensifying risk of flood wave propagation resulting from upstream dam failure. A failure initiated at Azad Dam, for instance, would likely generate a high-energy flood wave traversing the Gura and Sirwan Rivers. Given the scale and force of such a release, the downstream Daryan Dam may not withstand the surge, triggering a successive breach. This chain reaction would substantially amplify flood magnitude and momentum as it progresses toward Darbandikhan, elevating the risk of overtopping, rapid water level fluctuations, and structural loading.The severity of downstream impacts is governed by critical breach parameters such as time to failure, breach geometry, and peak discharge. Despite the evident threat posed by such cascading failures, there remains a significant gap in the literature concerning the cumulative hydrodynamic consequences on downstream infrastructures like Darbandikhan Dam. Addressing this research void, the present modeling effort offers new insights into the systemic vulnerabilities associated with compound dam failures in transboundary river systems.

2.3 HEC-RAS

This research utilizes the Hydrologic Engineering Center's River Analysis System (HEC-RAS) for hydrodynamic modeling, specifically versions 6.6 and 6.7 Beta, obtained from the official U.S. Army Corps of Engineers website (www.hec.usace.army.mil). HEC-RAS is an extensive, open-access software created by USACE that facilitates one-dimensional (1D) and two-dimensional (2D) hydraulic simulations for various applications, including steady and unsteady flow calculations, dam breach modeling, sediment transport, water quality evaluation, and the hydraulic analysis of structures like spillways and weirs **[27- 29]**. The user interface is crafted to be intuitive, facilitating efficient engagement with topography data, breach parameters, and flood simulation scenarios **[30, 31]**. This research models dam breach scenarios in the 2D domain of HEC-RAS, estimating breach parameters such as failure duration and average breach breadth using empirical formulations, including Froehlich's equations Specifically, the average breach width (B_{avg}) and breach formation time (T_f) were estimated using the following regression relations proposed by Froehlich (2008)

$$B_{avg} = 0.27\ K_o\ V_w^{0.32}\ H_b^{0.04} \quad \text{.....(1)}$$

$$T_f = \sqrt{\frac{V_w}{g h_b^{\,2}}} \quad \text{.....(2)}$$

where:

B_{avg} = average breach width (m)
K_o = coefficient (1.3 for overtopping, 1.0 for piping)
V_w = reservoir volume at time of failure (m^3)
h_b = height of the final breach (m)
g = gravitational acceleration (9.80665 m/s^2)
T_f = breach formation time (s).

Froehlich's regression equations are widely regarded as standard practice in dam breach modeling, and their reliability depends on accurate parameterization and application within valid conditions. The underlying dataset used to develop these regressions was based on dam failures with heights ranging from (3.05 to 92.96 m), with the majority of cases (< 30 m) being small to medium earthfill dams **[32, 33]**. These configurations provide comprehensive evaluations of downstream flood propagation, water surface elevations, peak discharge, and time-to-peak values, which are essential for assessing the potential consequences of dam failure incidents **[34, 35]**.

2.4 Terrain data

For hydraulic modeling and flood analysis, a 30-meter resolution Digital Elevation Model (DEM) was obtained from the Shuttle Radar Topography Mission (SRTM) dataset through the USGS Earth Explorer portal (https://earthexplorer.usgs.gov), which provides globally accessible topographic data **[36, 37]**. SRTM DEM provides globally consistent coverage, relatively higher vertical accuracy (~10–16 m RMSE), and extensive validation in hydrological and dam-break studies, making it the most appropriate choice for dam-break studies. The DEM data, aligned with WGS 1984 UTM Zone 38N, was truncated to encompass the geographic range between latitudes (34°N and 35°N) and longitudes (45°E and 46°E), thereby guaranteeing comprehensive coverage of the research area and surrounding catchments. The DEM was processed in ArcMap and transformed into a Triangulated Irregular Network (TIN) format to enable the delineation of river networks, floodplains, and cross sections utilizing HEC-GeoRAS tools, in accordance with methodologies employed in comparable studies **[38]**. The SRTM data utilized predates the building of the Azad Dam, enabling the implementation of a comprehensive dynamic wave routing technique instead of depending on simplified storage area estimations. This methodology enhances the precision of hydrodynamic modeling by facilitating a detailed depiction of flood wave propagation over natural terrain **[13]**. The topography data facilitate the extraction of essential geometric elements, including channel centerlines, bank alignments, and elevation profiles, required for constructing model geometry in HEC-RAS **[30]**.

2.5 Breach prediction models

A significant issue in dam failure modeling is the calculation of breach characteristics, which are fundamentally unpredictable. The breach location, size, and development time are regarded as the most unexpected elements **[39]**. To mitigate this uncertainty, numerous empirical and regression-based equations have been suggested in the literature. Models created by **[33, 40 - 44]**, and **Xu and Zhang 2009**, have gained extensive acceptance owing to their relevance to various dam types and collapse situations **[45].** These models generally associate breach parameters with accessible inputs, such as dam height, reservoir capacity, and failure method. For instance, whereas several methodologies concentrate just on beginning water

levels and failure volume, **Xu and Zhang** 's methodology integrates supplementary variables such as reservoir morphology, dam material erodibility, and structural classification, hence providing improved flexibility and accuracy **[44]**. Notwithstanding their prevalent application, it is crucial to acknowledge that over 75% of the data supporting these empirical models derives from dams under 15 meters in height, thus constraining forecast accuracy for taller structures **[33]. Froehlich**'s regression equations are commonly incorporated into dam break modeling platforms like HEC-RAS, especially for calculating average breach and formation time. The **Froehlich**'s model incorporates both the start and advancement phases of erosion, yielding more conservative estimates of breach development time than alternative formulations **[43, 46]**. The choice of breach prediction models must correspond to the physical environment and scale of the dam being evaluated.

2.6 Dam Failure Scenarios

Four breach scenarios were designed to evaluate the transboundary flood risk posed by upstream dam failures on Darbandikhan Dam. The simulations incorporate two failure mechanisms piping and overtopping initiated at Azad Dam and leading to successive failures of Daryan and Hirwa Dams. Storage volumes were assigned as shown in Table 2. The four scenarios represent combinations of breach mechanisms and Darbandikhan's storage level: full supply level (FSL) and semi-full level.

S1: Azad Dam failure by overtopping → cascading overtopping failures downstream; Darbandikhan at FSL.

S2: Azad Dam failure by piping → cascading overtopping failures downstream; Darbandikhan at FSL.

S3: Azad Dam failure by overtopping → cascading overtopping failures downstream; Darbandikhan semi-full.

S4: Azad Dam failure by piping → cascading overtopping failures downstream; Darbandikhan semi-full.

This framework enables quantification of downstream impact sensitivity to initial hydraulic conditions.

3 Results and Discussion

3.1 Scenarios Description

To evaluate the potential for cascading hydraulic failures within the (Azad–Daryan–Hirwa) dams' system and its downstream implications for Darbandikhan Dam, four initial breach scenarios were formulated. These scenarios incorporate two key failure initiation modes overtopping and piping (internal erosion) across two reservoir conditions at Darbandikhan: full supply level (FSL) and partially filled (semi-full). Among these, two representative cases were prioritized for detailed simulation and analysis, selected on the basis of their severity, operational realism, and capacity to generate significant flood wave propagation and structural risk downstream.

Scenario 1: Full-Capacity Sequential Overtopping

This case simulates a progressive failure initiated by overtopping at Azad Dam, followed sequentially by overtopping-induced breaches at Daryan and Hirwa Dams. During this sequence, Darbandikhan Dam is assumed to be at its full storage level of 2.55 billion cubic meters, with a corresponding water surface elevation of 485 m. The scenario is intended to represent a high-intensity cascading flood under peak hydrologic loading conditions, allowing for the assessment of rapid wave arrival, maximum discharge volumes, and the limits of flood attenuation within the Darbandikhan reservoir.

Scenario 2: Mixed-Mode Breach with Full Reservoir Load

In this configuration, the failure process is initiated by a piping breach at Azad Dam, resulting in downstream overtopping failures at both Daryan and Hirwa Dams. Similar to Scenario 1, Darbandikhan is maintained at full capacity (2.55 billion m^3, WSE = 485 m) to examine the response of the downstream system under compounded structural and hydrodynamic stress. This scenario enables investigation of the influence of breach mechanism type on flood hydrograph evolution, time to peak, and resultant pressures on downstream reservoir operations. These scenarios are designed to reflect plausible high-risk conditions within a seismically and hydrologically sensitive transboundary basin, offering insight into potential failure sequences and their broader implications for dam safety management and emergency preparedness.

3.2 Water Surface Elevation Comparison at Critical Locations

Table 3 presents the peak water surface elevations (WSEs) recorded at two hydraulically significant locations: the entry point of breach flows at the Iraq–Iran border, marking the upstream boundary of the Darbandikhan reservoir, and the immediate vicinity upstream of the dam structure itself. These measurements allow for a comparative evaluation of flood attenuation as water propagates through the reservoir. The WSE values at the transboundary entry reflect the intensity of the incoming flood wave, whereas those near the dam indicate the degree to which the reservoir absorbs and moderates that energy. The difference between these two readings provides insight into the reservoir's buffering performance under various failure scenarios. This analysis supports the optimization of reservoir operating levels and informs real-time emergency protocols, particularly regarding controlled drawdown strategies and gate operations during extreme inflow events.

3.3 Water Surface Elevation Rise and Flood Arrival Dynamics

An initial comparison of breach hydrographs generated for piping and overtopping failure modes at Azad Dam revealed only minor differences in key hydraulic parameters, including peak discharge, flood wave travel time, and total outflow volume. Given the relatively modest divergence between the two failure mechanisms,

subsequent hydraulic and geotechnical analyses focus primarily on overtopping-induced scenarios. In particular, Scenario 1 and Scenario 2 are prioritized, as they represent the most critical configurations in terms of downstream flood impact, rapid wave propagation, and potential structural instability at Darbandikhan Dam. In Scenario 1, a cascade overtopping failure commences at Azad Dam, with all upstream dams (Azad, Daryan, and Hirwa) at maximum storage capacity, and the Darbandikhan Reservoir is also presumed to be at full capacity (starting WSE = 485.0 m). After the overtopping breach of Azad Dam, the flood wave swiftly advances downstream, reaching Daryan Dam in roughly 103 minutes. Subsequently, the Daryan Dam fails due to overtopping 25 minutes later, specifically 128 minutes after the Azad failure. The combined flood wave then advances toward Hirwa Dam. Inundation of the upstream Hirwa valley begins around 143 minutes post-failure, with full submergence occurring by 168 minutes. The flood wave continues its path downstream, reaching the Iraq border approximately 194 minutes after the initial breach of Azad Dam. At this location, the water surface elevation rises sharply from 485.0 m to approximately 512.0 m. By 207 minutes, the flood wave reaches the main body of Darbandikhan Dam, where water levels begin to rise and eventually reach 491.55 m at 345 minutes post-failure. Due to the rapid and substantial increase in reservoir level, water begins to overflow the spillway gates of Darbandikhan Dam set at a crest elevation of 485.0 m causing significant outflow and flooding in downstream areas. Simultaneously, the bottom outlet is operated at full capacity to discharge the maximum possible flow in an effort to reduce reservoir levels and preserve the structural safety of the dam. These emergency releases, while essential for dam integrity, contribute to heightened downstream flood risk and demand urgent risk management interventions.

3.4 Impact on Downstream Areas of Azad and Daryan, Hiwa Dams, in Iran

The cascading overtopping scenario results in severe flooding, particularly in the valleys located between Azad and Hirwa dams. The initial failure of Azad dam due to overtopping generates a high-velocity flood wave that rapidly propagates through the narrow river valleys, overwhelming the storage capacity of Daryan dam and causing its subsequent failure. The combined discharge from both dams substantially elevates upstream water surface levels and increases flow velocities throughout the interconnected streams. Hydraulic modeling indicates that over 16 villages situated between Azad and Hirwa reservoirs are critically affected by the flood wave. In particular, the stretch between Azad dam and Hirwa dam contains a concentration of rural settlements where over 1,000 houses are expected to be submerged or severely damaged by the cascading flood wave. Notably, Hirwa Village, located just upstream of Hirwa Dam (Figure 7), is projected to be completely submerged, with approximately 40 houses and an estimated 125 residents inundated under flood depths exceeding 22 meters. As shown in (Figure 8), widespread inundation also impacts the surrounding agricultural lands, which serve as the primary source of livelihood for the affected communities. Due to the steep topography and narrow shape of the river valleys, the velocity of floodwaters following Additionally, the floodwaters submerge key regional roads that connect upstream villages, effectively severing transport and communication links. This loss of connectivity poses major challenges to emergency response, aid delivery, and long-term recovery, further compounding the social and economic vulnerability of the impacted population. Location of dams and villages are shown in (Figure 9).

3.5 Impact on Downstream Areas, in Iraq

Beyond the Hirwa Dam, the cascading flood wave progresses into northeastern Iraq, generating severe transboundary hydrodynamic impacts. Model simulations reveal that at least 12 Iraqi villages lie within the projected inundation zone. These include Soila Mesh, Kalwran, Berashka, Dolash, Qajir, Grdi Sharif, Qoitas, Tapakal, Suwary, Hayas, Kani Shekh, and Kawchktash. Many of these settlements are predominantly agriculture-based communities, rendering them highly vulnerable to flood-induced socioeconomic disruption, infrastructure destruction, and population displacement. In addition to the direct impact on rural settlements, over 70 km² of agricultural land primarily located upstream of Darbandikhan Dam near Halabja city and the Said Sadiq and Sirwan regions is expected to be submerged. This widespread inundation poses a serious threat to food security and rural livelihoods in the affected areas. Furthermore, the recently constructed highway connecting Halabja city to the adjacent districts is forecasted to be overtopped by floodwater see (Figure 10), exacerbating transportation difficulties and obstructing emergency response and recovery operations during and after the flood event. The spatial extent and inundation depth affecting these downstream communities are illustrated in (Figure 11), and (Figure 12), reflecting the full magnitude of the cascading failure event's impact.

3.6 Sediment Transport and morphodynamical Impact

The extraordinarily high flood velocities recorded during the simulation ranged from (10 m/s - 25 m/s) indicate severe sediment transport potential. As represented by the Hjulström diagram (Figure 13), these velocities are sufficient to erode and mobilize all classes

of sediment particles, including coarse gravels and boulders. Such high-energy flows are likely to cause extensive riverbed scouring, embankment erosion, and widespread morphological changes in both upstream valleys and the Darbandikhan reservoir inlet zone see (Figure 14), and (Figure 15). Furthermore, the intense hydraulic force associated with these velocities has the capacity to uproot trees, destroy agricultural farms, and strip topsoil, thereby devastating local food production systems and degrading arable land. This aligns with sediment transport theory, which holds that critical erosion velocities for even the coarsest particles are exceeded under such extreme hydraulic conditions **[47]**. These geomorphic responses can significantly impair water quality, reduce reservoir storage capacity, and destabilize aquatic habitats in the medium to long term.

4 Discussion

Cascading Failure Dynamics and Wave Propagation

The simulation results highlight the critical implications of cascading dam failures within the (Azad–Daryan–Hirwa–Darbandikhan) system. Scenario 1 (sequential overtopping) and Scenario 2 (Pipping failure) both result in rapid flood wave generation and downstream propagation; however, Scenario 1 represents the most severe condition, with all upstream dams overtopped under full storage conditions and Darbandikhan Dam at maximum capacity (WSE = 485.0 m). The breach of Azad Dam triggers a wave that reaches Daryan Dam in 103 minutes, initiating its failure by overtopping 25 minutes later. The subsequent failure of Hirwa Dam occurs as the flood arrives within 143 minutes, with full submergence of huge areas by 168 minutes. The rapid arrival time and cumulative discharge from all three failed reservoirs demonstrate a highly aggressive wavefront that challenges the hydraulic buffering capacity of Darbandikhan Reservoir.

Reservoir Response and Water Surface Elevation Trends.

Water surface elevation (WSE) data extracted at the Iran–Iraq border and near Darbandikhan Dam body offer valuable insights into the attenuation behavior of the Darbandikhan Reservoir. Under Scenario 1, WSE at the border peak at 512.0 m an increase of 27 meters above the initial reservoir level before gradually reducing to 491.55 m near the dam structure due to partial attenuation. In Scenario 2, slightly lower elevations (510.31 m at the border, 490.08 m near the dam) were observed, confirming that piping-induced breaches generate marginally less severe hydraulic loads. Nonetheless, both scenarios exceed the spillway gates elevation, confirming that overflow is inevitable and safety interventions are urgently required.

Emergency Discharge and Structural Risk at Darbandikhan Dam

Once the flood wave reaches Darbandikhan Dam (207 minutes post-initial breach), water begins to overflow the gated spillways, which are set at 485.0 m elevation. By 345 minutes, the WSE has risen to 491.55 m, surpassing both the Full Supply Level and operational thresholds, floodwater will also overflow the gates without control. To mitigate structural risk, the bottom outlet is activated to discharge flow at maximum capacity. While this action is vital for preserving dam integrity, it significantly contributes to downstream flooding. Thus, the dam transitions from a passive buffer to an active contributor to downstream hazard, underscoring the importance of synchronized gate operation and emergency planning.

Impacts on Upstream Iranian Communities

The valleys between Azad, Daryan, and Hirwa dams bear the brunt of the flood impact, especially under Scenario 1. The narrow, steep-sided topography amplifies flow velocity ranging from (10 m/s to 25 m/s) leading to extreme erosion and sediment transport. Hirwa Village, located upstream of Hirwa Dam, is fully submerged, with 40 residential structures and an estimated 125 residents affected. Adjacent agricultural lands are also inundated. The velocity range surpasses critical thresholds for sediment entrainment, including boulders and coarse gravel, leading to riverbed degradation and irreversible morphological changes. These geomorphological impacts threaten farmland productivity, which is the economic backbone of many affected settlements. In addition, the destruction of rural infrastructure, including inter-village roads and bridges, further isolate these communities and impairs disaster response logistics. The cascading nature of the failure, compounded by limited lead time, suggests that many upstream villages would have little to no warning before being inundated.

Transboundary Impacts in Northeastern Iraq

Once beyond Hirwa Dam, the flood wave crosses into Iraq, producing extensive downstream inundation. The flood affects at least 12 villages such as Soila Mesh, Kalwran, Berashka, Dolash, Qajir, and others mostly agricultural in nature. Over 70 km² of farmland near Halabja, Said Sadiq, and Sirwan is submerged, threatening food security and income for thousands of residents. Infrastructure is also heavily impacted the submergence of Halabja's newly constructed highway, with water depths exceeding 2 meters. This isolation compounds post-flood recovery efforts and delays aid delivery. The severity of these impacts confirms that cascading dam failures not only present national hazards but also transboundary threats, necessitating joint disaster management strategies between Iran and Iraq.

Sediment Transport and Morphological Consequences

The hydraulic velocities observed in both upstream valleys and near the reservoir inlet of Darbandikhan are high enough to mobilize a broad spectrum of sediment sizes, from fine clays to large cobbles. According to the Hjulström diagram, which defines erosion and

deposition thresholds based on particle size and flow velocity, velocities exceeding 1500 cm/s (15 m/s) will entrain and transport virtually all sediment classes **[47]**. These high-energy flows result in riverbed incision, floodplain stripping, and siltation at critical downstream zones, which may reduce reservoir capacity and compromise future water quality.

5 Conclusion

This study presents a detailed hydrodynamic analysis of cascading dam failure scenarios involving the Azad, Daryan, and Hirwa dams, with particular emphasis on their downstream impacts on Darbandikhan Dam in Iraq. Two principal scenarios were evaluated Scenario 1 (sequential overtopping at full capacity) and Scenario 2 (piping at Azad Dam followed by overtopping at downstream dams). Both scenarios demonstrated the vulnerability of the interconnected reservoir system to extreme flood events, especially under full reservoir conditions. Scenario 1 emerged as the most critical case, producing rapid wave propagation, minimal attenuation, and the highest flood loads at the Iraq–Iran border and near Darbandikhan Dam. Water surface elevation at the border peaked at 512.0 m, while near the dam structure it rose to 491.55 m, far exceeding the spillway crest elevation of 485.0 m. The flood wave overtopped spillway of Darbandikhan Dam, triggering emergency discharges through the bottom outlet to preserve structural safety.
though at the cost of increased downstream flooding. The cascading failure resulted in catastrophic impacts both upstream in western Iran and downstream in northeastern Iraq. Over 16 Iranian villages and 12 Iraqi villages were affected, with Hirwa Village experiencing complete submergence. Approximately 72.84 km² of land including productive agricultural areas and transportation infrastructure was inundated. Flow velocities ranging from (10 m/s to 25 m/s) exceeded critical sediment entrainment thresholds, indicating severe erosion, sediment transport, and long-term geomorphological changes.

6 Recommendations

To mitigate the risks identified in the dam failure simulations, several key measures are proposed:
1. Structural and Operational Improvements: Implement dynamic reservoir drawdown strategies during high-risk periods and upgrade the spillway and outlet capacities at Darbandikhan Dam to handle cascading flood inflows.
2. Early Warning and Monitoring: Establish real-time flood monitoring systems upstream of Azad Dam, develop rapid alert protocols for downstream communities, and provide flood response training and evacuation planning for vulnerable villages.
3. Transboundary Coordination: Strengthen cooperation between Iran and Iraq through bilateral agreements, shared hazard mapping tools, and joint emergency response planning and drills.
4.Future Research Needs: Investigate sedimentation and siltation effects, analyze slope stability risks under rapid hydraulic changes, and incorporate climate resilience into dam safety strategies.

References

[1] Amini, Ata; Arya, Alborz; Eghbalzadeh, Afshin; Javan, Mitra. 2017. Peak flood estimation under overtopping and piping conditions at Vahdat Dam, Kurdistan, Iran. Arabian Journal of Geosciences, 10: 2854. doi:10.1007/s12517-017-2854-y.

[2] Cannata, M.; Marzocchi, R. 2012. Two-dimensional dam break flooding simulation: a GIS-embedded approach. Natural Hazards, 61: 1143–1159. doi:10.1007/s11069-011-9974-6.

[3] Wu, Weiming; Altinakar, Mustafa; Al-Riffai, Mahmoud; Bergman, Nathaniel; Bradford, Scott; Cao, Zhixian; Chen, Qin; Constantinescu, George; Duan, Jennifer; Gee, D.; Greimann, Blair; Hanson, Greg; He, Zhiguo; Hegedus, Pal; Hoestenberghe, —. 2011. Earthen embankment breaching. Journal of Hydraulic Engineering, 137(12). doi:10.1061/(ASCE)HY.1943-7900.0000498.

[4] Brunner, G. W. 2016. HEC-RAS River Analysis System, User's Manual (Version 5.0). U.S. Army Corps of Engineers, Hydrologic Engineering Center, Davis, CA. (online). Accessed May 13, 2025. Available at: https://www.hec.usace.army.mil/software/hec-ras/documentation/HEC-RAS%205.0%20Users%20Manual.pdf

[5] Bosa, S.; Petti, M. 2013. A numerical model of the wave that overtopped the Vajont Dam in 1963. Water Resources Management, 27: 1763–1779. doi:10.1007/s11269-012-0162-6.

[6] Li, Yanlong; Tian, Chao; Wen, Lifeng; Chen, Anke; Wang, Lin; Qiu, Wen; Zhou, Heng. 2021. A study of the overtopping breach of a sand-gravel embankment dam using experimental models. Engineering Failure Analysis, Vol. 124: 105360.

[7] ICOLD. 1998. Bulletin 111: Global Climate Change – Impacts on Water Resources and Dam Safety. International Commission on Large Dams, Paris. (online). Accessed May 01, 2025. Available at: https://www.icold-cigb.org

[8] Singh, J.; Altinakar, M. S.; Ding, Y. 2011. Two-dimensional numerical modeling of dam-break flows over natural terrain using a central explicit scheme. Advances in Water Resources, 34(10): 1366–1375. doi:10.1016/j.advwatres.2011.07.007.

[9] Qi, H.; Altinakar, M. S. 2012. GIS-based decision support system for dam break flood

management under uncertainty with two-dimensional numerical simulations. Journal of Water Resources Planning and Management (online). Accessed May 28, 2025. Available at: https://ascelibrary.org/doi/10.1061/(ASCE)WR.1943-5452.0000192.

[10] Álvarez, M.; Puertas, J.; Peña, E. 2017. Two-dimensional dam-break flood analysis in data-scarce regions: The case study of Chipembe Dam, Mozambique. Water, 9(6): 432. (online). Accessed May 28, 2025. Available at: https://www.mdpi.com/2073-4441/9/6/432.

[11] Kumar, S.; Jaswal, A.; Pandey, A.; Sharma, N. 2017. Literature review of dam break studies and inundation mapping using hydraulic models and GIS. International Journal of Engineering Research and Applications, 4(5).

[12] Fread, D. L. 1984. DAMBRK: The NWS Dam-Break Flood Forecasting Model. Hydrologic Research Laboratory, National Weather Service, NOAA.

[13] USACE. National Inventory of Dams. (online). U.S. Army Corps of Engineers. Available at: http://geo.usace.army.mil/pgis/p?p14397:5:0:NO.

[14] Yu, S.; et al. 2021. Study of the Sheyuegou dam breach – Experience with the post-failure investigation and back analysis. Engineering Failure Analysis, 125: 105441. doi:10.1016/j.engfailanal.2021.105441.

[15] Butt, M. J.; Umar, M.; Qamar, R. 2013. Landslide dam and subsequent dam-break flood estimation using HEC-RAS model in Northern Pakistan. Natural Hazards, 65(1). doi:10.1007/s11069-012-0361-8.

[16] Sharma, P.; Mujumdar, S. Dam break analysis using HEC-RAS and HEC-GeoRAS – A case study of Ajwa Reservoir. ResearchGate (online). Accessed May 28, 2025. Available at: https://www.researchgate.net/publication/314273997_Dam_Break_Analysis_Using_HEC-RAS_and_HEC-GeoRAS_-_A_Case_Study_of_Ajwa_Reservoir.

[17] Joshi, M. M.; S. S. S. 2017. Two-dimensional dam break flow study using HEC-RAS for Ujjani Dam. International Journal of Engineering and Technology, 9(4): 2923–2928. doi:10.21817/ijet/2017/v9i4/170904032.

[18] Albu, L. M.; Enea, A.; Iosub, I. G.; Breaban, M. 2020. Dam breach size comparison for flood simulations: A HEC-RAS based, GIS approach for Drăcșani Lake, Sitna River, Romania. Water, 12(4): 1090. (online). Accessed May 28, 2025. Available at: https://www.mdpi.com/2073-4441/12/4/1090.

[19] Albu, L. M.; Enea, A.; Stoleriu, C. C.; Niacșu, L. G.I.S. implementation on dam-break flood vulnerability analysis – A case study of Cătămărăști Dam, Botoșani, Romania. ResearchGate (online). Accessed May 28, 2025. Available at: https://www.researchgate.net/publication/334063213_GIS_Implementation_on_Dam-Break_Flood_Vulnerability_Analysis_-_A_Case_Study_of_Catamarasti_Dam_Botosani_Romania.

[20] Kilania, S.; Chahar, B. R. 2019. A dam break analysis using HEC-RAS. Proceedings of the World Environmental and Water Resources Congress. (online). Accessed May 28, 2025. Available at: https://ascelibrary.org/doi/10.1061/9780784482353.036.

[21] Aribawa, T. M. 2021. Assessment of flood propagation due to several dams break in Banten Province. Academia.edu (online). Accessed May 28, 2025. Available at: https://www.academia.edu/99747382/Assessment_of_Flood_Propagation_Due_to_Several_Dams_Break_in_Banten_Province.

[22] Zaidan, K.; Omed, Y.; Alshkane, Y.; Khani, A.; Hama, S. K. 2019. Performance of Darbandikhan Dam during a major earthquake on November 12, 2017.

[23] MohabQuds.co. Azad Dam. (online). Accessed May 28, 2025. Available at: http://mahabghodss.net/ExternalSites/new/PrjDtl.aspx?ID=69.

[24] Chomani, K.; Bijnens, T. 2016. The impact of the Daryan Dam on the Kurdistan Region of Iraq.

[25] Jamshidi, A.; Sedaghatnia, M.; Sabzevari, K. M. 2021. The role of structural factors in directing methane and carbon dioxide to the Nosud water transmission tunnel (Azgeleh – northwest of Kermanshah). New Findings in Applied Geology, June 2021. doi:10.22084/nfag.2020.21511.1417.

[26] Faraj, D.; Kawa, Z. A. 2020. The impact of the Tropical Water Project on Darbandikhan Dam and Diyala River Basin. Academia.edu (online). Accessed May 28, 2025. Available at: https://www.academia.edu/43498582/The_Impact_of_the_Tropical_Water_Project_on_Darbandikhan_Dam_and_Diyala_River_Basin_A_R_T_I_CL_E_I_N_F_O.

[27] Brunner, G. W. 2014. HEC-RAS River Analysis System: Hydraulic Reference Manual (Version 4.0). U.S. Army Corps of Engineers, Hydrologic Engineering Center, Davis, CA.

[28] Dasallas, L.; Kim, Y.; An, H. 2019. Case study of HEC-RAS 1D–2D coupling simulation: 2002

Baeksan flood event in Korea. Water, 11(10): 2048. (online). Accessed May 30, 2025. Available at: https://www.mdpi.com/2073-4441/11/10/2048.

[29] Bui, D. T.; Asl, D. T.; Ghanavati, E.; Al-Ansari, N.; Khezri, S. 2020. Effects of inter-basin water transfer on water flow condition of destination basin. Sustainability, 12(1): 338. (online). Accessed May 30, 2025. Available at: https://www.mdpi.com/2071-1050/12/1/338.

[30] Ghindaoanu, V. B.; Hutanu, E.; Urzica, A. 2019. The GIS modeling of the terrain favorability for the placement of constructions in the areas with hydro-geomorphological risk. Proceedings of the International Conference Geobalcanica 2018, pp. 21–30. doi:10.18509/GBP.2018.03.

[31] Costabile, P.; Costanzo, C.; Ferraro, D.; Macchione, F.; Petaccia, G. 2020. Performances of the new HEC-RAS version 5 for 2-D hydrodynamic-based rainfall-runoff simulations at basin scale: Comparison with a state-of-the-art model. Water, 12(9): 2326. doi:10.3390/w12092326.

[32] Mihu-Pintilie, A.; Cîmpianu, C. I.; Stoleriu, C. C.; Pérez, M. N.; Paveluc, L. E. 2019. Using high-density LiDAR data and 2D streamflow hydraulic modeling to improve urban flood hazard maps: A HEC-RAS multi-scenario approach. Water, 11(9): 1832. (online). Accessed May 30, 2025. Available at: https://www.mdpi.com/2073-4441/11/9/1832.

[33] Brunner, G. W. 2016. HEC-RAS River Analysis System: Hydraulic Reference Manual (Version 5.0). U.S. Army Corps of Engineers, Hydrologic Engineering Center, Davis, CA.

[34] Patel, D.; Ramirez, J.; Srivastava, P. K.; Bray, M.; Han, D. 2017. Assessment of flood inundation mapping of Surat city by coupled 1D/2D hydrodynamic modeling: A case application of the new HEC-RAS 5. Natural Hazards, 89(1): 93–130. doi:10.1007/s11069-017-2956-6.

[35] West, M.; Morris, M.; Hassan, M. 2018. A guide to breach prediction. Dams and Reservoirs, 28(4): 150–152. doi:10.1680/jdare.18.00031.

[36] Shawky, M.; Moussa, A.; Hassan, Q.; El-Sheimy, N. 2019. Pixel-based geometric assessment of channel networks/orders derived from global spaceborne digital elevation models. Remote Sensing, 11(3): 235. doi:10.3390/rs11030235.

[37] Niipele, J. N.; Chen, J. 2019. The usefulness of ALOS-PALSAR DEM data for drainage extraction in semi-arid environments in the Iishana sub-basin. Journal of Hydrology: Regional Studies, 21: 57–67. doi:10.1016/j.ejrh.2018.11.003.

[38] Vertex ASF. ASF Data Search. Alaska Satellite Facility (online). Accessed May 30, 2025. Available at: https://search.asf.alaska.edu/#/.

[39] Gee, D. M. 2012. Dam breach modeling with HEC-RAS using embankment erosion process models. Proceedings of the World Environmental and Water Resources Congress 2012, pp. 1347–1356. (online). Accessed May 1, 2025. Available at: https://ascelibrary.org/doi/10.1061/41114(371)144.

[40] Von Thun, J.; Lawrence, J. 1990. Guidance on breach parameters. Internal Memorandum, U.S. Department of the Interior, Bureau of Reclamation, Denver, CO. (online).

[41] Froehlich, D. 2008. Embankment dam breach parameters and their uncertainties. Journal of Hydraulic Engineering, 134(12): 1708–1721. doi:10.1061/(ASCE)0733-9429(2008)134:12(1708).

[42] Pierce, M.; Thornton, C.; Abt, S. 2010. Predicting peak outflow from breached embankment dams. Journal of Hydraulic Engineering, 15(5): 338–349. doi:10.1061/(ASCE)HE.1943-5584.0000197.

[43] Froehlich, D. 2016. Predicting peak discharge from gradually breached embankment dam. Journal of Hydraulic Engineering, 21(9): 04016041. doi:10.1061/(ASCE)HE.1943-5584.0001424.

[44] Xu, Y.; Zhang, L. M. 2009. Breaching parameters for earth and rockfill dams. Journal of Geotechnical and Geoenvironmental Engineering, 135(12): 1957–1970. (online). Accessed May 1, 2025. Available at: https://ascelibrary.org/doi/10.1061/(ASCE)GT.1943-5606.0000162.

[45] Psomiadis, E.; Tomanis, L.; Kavvadias, A.; Soulis, K.; Charizopoulos, N.; Michas, S. 2021. Potential dam breach analysis and flood wave risk assessment using HEC-RAS and remote sensing data: A multicriteria approach. Water, 13(3): 364. doi:10.3390/w13030364.

[46] Froehlich, D. 2016. Empirical model of embankment dam breaching. In Erosion in Geomechanics Applied to Dams and Levees, pp. 1826. CRC Press. doi:10.1201/9781315644479-285.

[47] Panchuk, K. 2023. Physical Geology – H5P Edition. H5P ed. Simple Book Publishing. (online). Accessed May 28, 2025. Available at: https://opentextbc.ca/physicalgeologyh5p.

انتشار فشل متعدد للسدود في نظام نهري عابر للحدود: دراسة حالة لسلسلة سدود آزاد–داريان–هيروا–دربندخان

المستخلص

تبحث هذه الدراسة في الآثار الهيدروديناميكية لانهيارات السدود المتتابعة ضمن شبكة خزانات مائية عابرة للحدود تشمل سدود آزاد، داريان، وهيروا في غرب إيران، وتأثيراتها على سد دربندخان في شمال شرق العراق. تم استخدام النمذجة ثنائية الأبعاد في برنامج HEC–RAS 6.6 لتطوير أربع سيناريوهات لانهيار السدود، مع تحليل تفصيلي لحالتين رئيسيتين هما الانهيار المتتابع الناتج عن فيضان القمة، والانهيار المختلط. أظهرت المحاكاة أن السيناريو الأول، الذي يتضمن فيضان القمة بكامل السعة، يشكل أعلى مستوى من الخطورة، حيث تنتقل موجات الفيضان بسرعة عبر الوديان الضيقة، مسببة ارتفاعات قصوى في منسوب سطح المياه تصل إلى ٥١٢.٠ متر عند الحدود الإيرانية – العراقية، و٤٩١.55 متر بالقرب من سد دربندخان، متجاوزة بوابات المفيض المضبوطة عند ٤٨٥.٠ متر. تشير التقديرات إلى غمر أكثر من ١٠٠٠ منزل بين سدود آزاد وداريان وهيروا، مع غمر قرية هيروا بالكامل تحت أعماق فيضانية تتجاوز ٢٢ متراً. وفي الجزء العراقي من الحوض، يتوقع غمر ما لا يقل عن ١٢ قرية بأعماق فيضانية تتجاوز ٢.٥ متر، بالإضافة إلى تأثر أكثر من ٧٠ كم٢ من الأراضي الزراعية، بما في ذلك البنية التحتية الحيوية مثل الطريق السريع في حلبجة، الذي يغمره أكثر من ٢ متر من مياه الفيضان. تتراوح سرعات الجريان بين ١٠ و٢٥ م/ث، وهي قيم تتجاوز حدود جرف الرواسب، مما يشير إلى احتمالية حدوث تآكل كبير، ونقل للرواسب، وآثار مورفولوجية طويلة الأمد على ضفاف الخزانات وقنوات التصريف. وتؤكد النتائج على الحاجة الماسة إلى تحسينات إنشائية، وبروتوكولات تشغيل ديناميكية للخزانات، وأنظمة مراقبة آنية، والتنسيق الطارئ عبر الحدود. كما تسلط الدراسة الضوء على أهمية دمج العوامل الجيومورفولوجية والمناخية في استراتيجيات سلامة السدود المستقبلية.

الكلمات المفتاحية:

HEC–RAS ، انهيار السد ، استقرار السد، خريطة الغمر، خريطة مخاطر الفيضانات.

Table (1) Azad, Daryan, Hirwa and Darbandikhan dam's properties

Items	Azad Dam	Daryan Dam	Hirwa Dam	Darbandikhan Dam
Dam Type	Rock-fill dam	Rockfill dam	Concrete dam	Rockfill dam
Height	115 m	169 m	45 m	128 m
Crest Elevation	1480m	710 m	660 m	495 m
Maximum WSE	1474m	705 m	654 m	485 m
Reservoir Capacity	300 million m3	316.3 million m3	12 million m3	2.55 billion m3

Table (2) Dams Storage according to Scenarios

Scenario	Initial Trigger	Azad Volume (10^6 m3)	Daryan Volume (10^6 m3)	Hirwa Volume (106 m3)	Darbandikhan State	Darbandikhan Volume (10^6 m3)	Darbandikhan Elevation (m)
S1	Overtopping Failure	300	316.3	12	Full	2550	485
S2	Piping Failure	360	316.3	12	Full	2550	485
S3	Overtopping Failure	300	316.3	12	Semi-Full	2050	480
S4	Piping Failure	360	316.3	12	Semi-Full	2050	480

Table (3) WSE results for each Scenarios

Location	Scenario 1 : WSE(m) Overtopping	Scenario 2 : WSE(m) Pipping
At Iran-Iraq Border	512.0	510.31
Near Darbandikhan Dam body	491.55	490.08

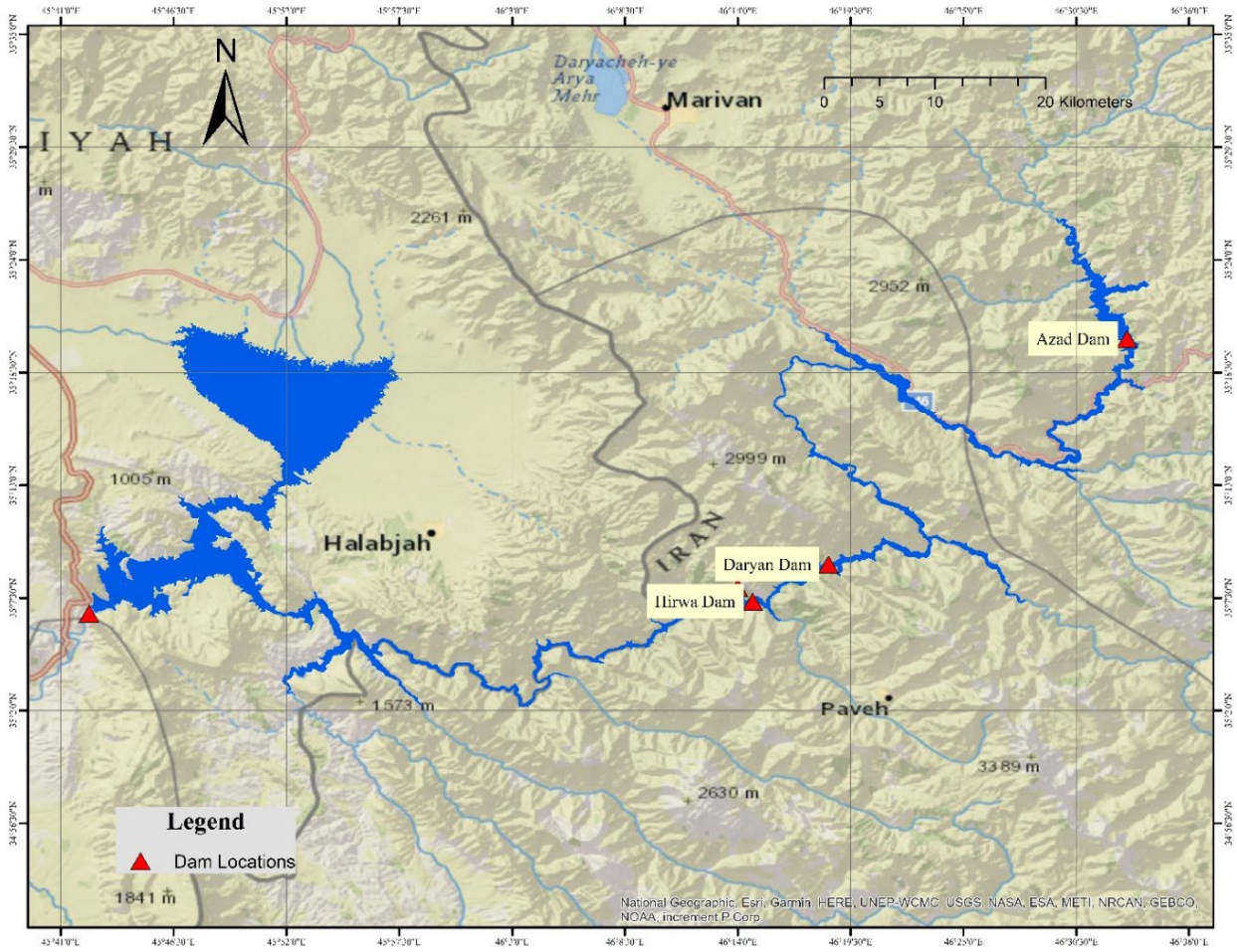

Fig. (1): Location map of Darbandikhan, Azad, Daryan and Hirwa dams.

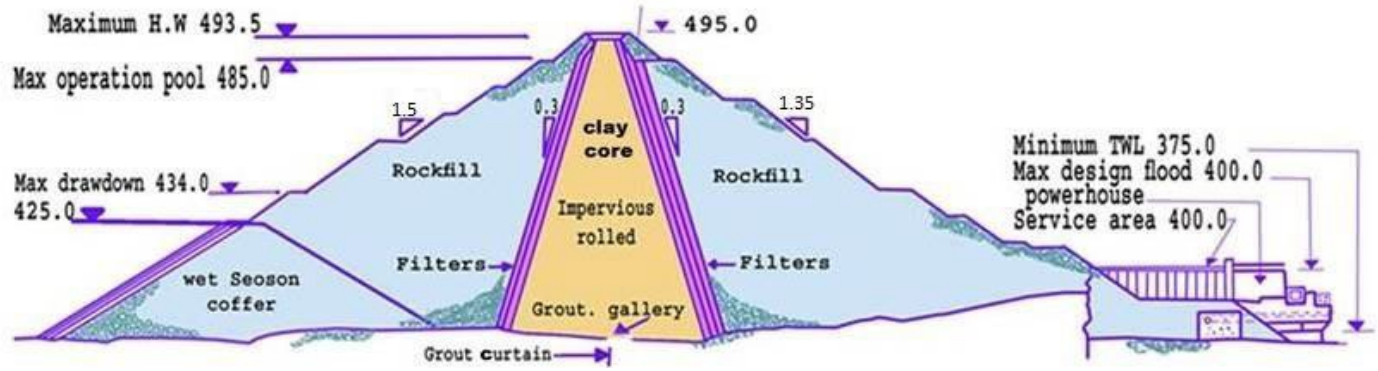

Fig. (2): Maximum cross section of the Darbandikhan Dam (Adopted from the Darbandikhan Dam Directorate)

Fig. (3): Azad dam

Fig. (4): Upstream view of Daryan dam **[24]**.

Fig. (5): Hirwa Dam looking upstream.

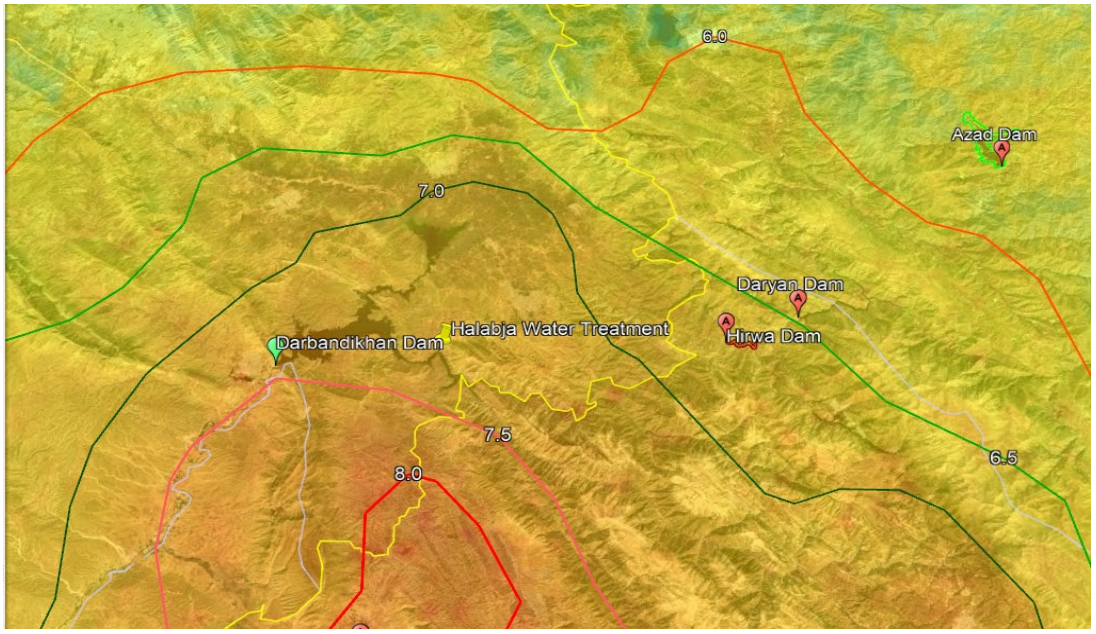

Fig. (6): Seismic contour map of the study area.

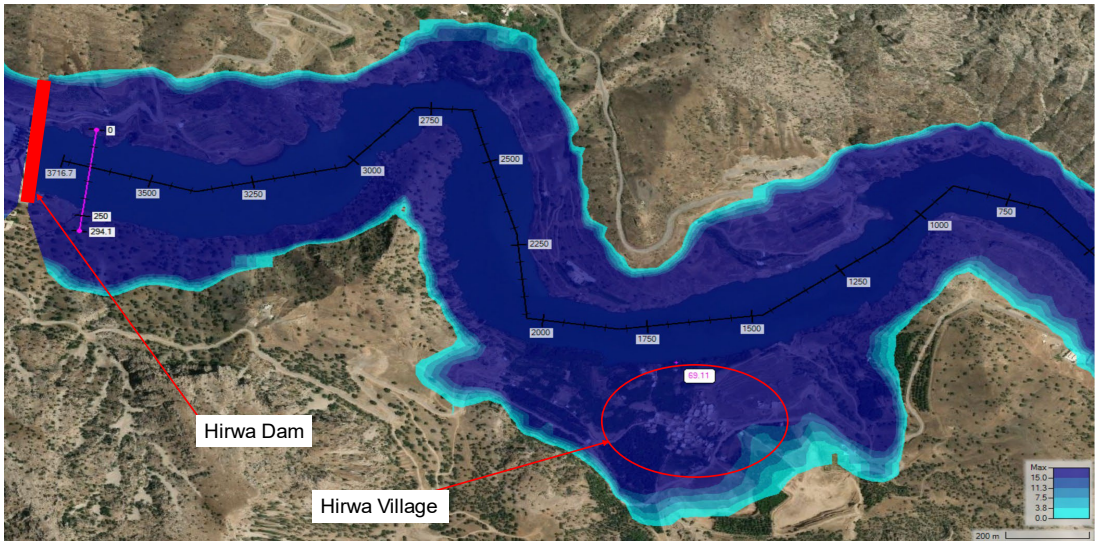

Fig. (7): Hirwa Village submergence after the flood.

Fig. (8): Houses are expected to be affected by the Flood.

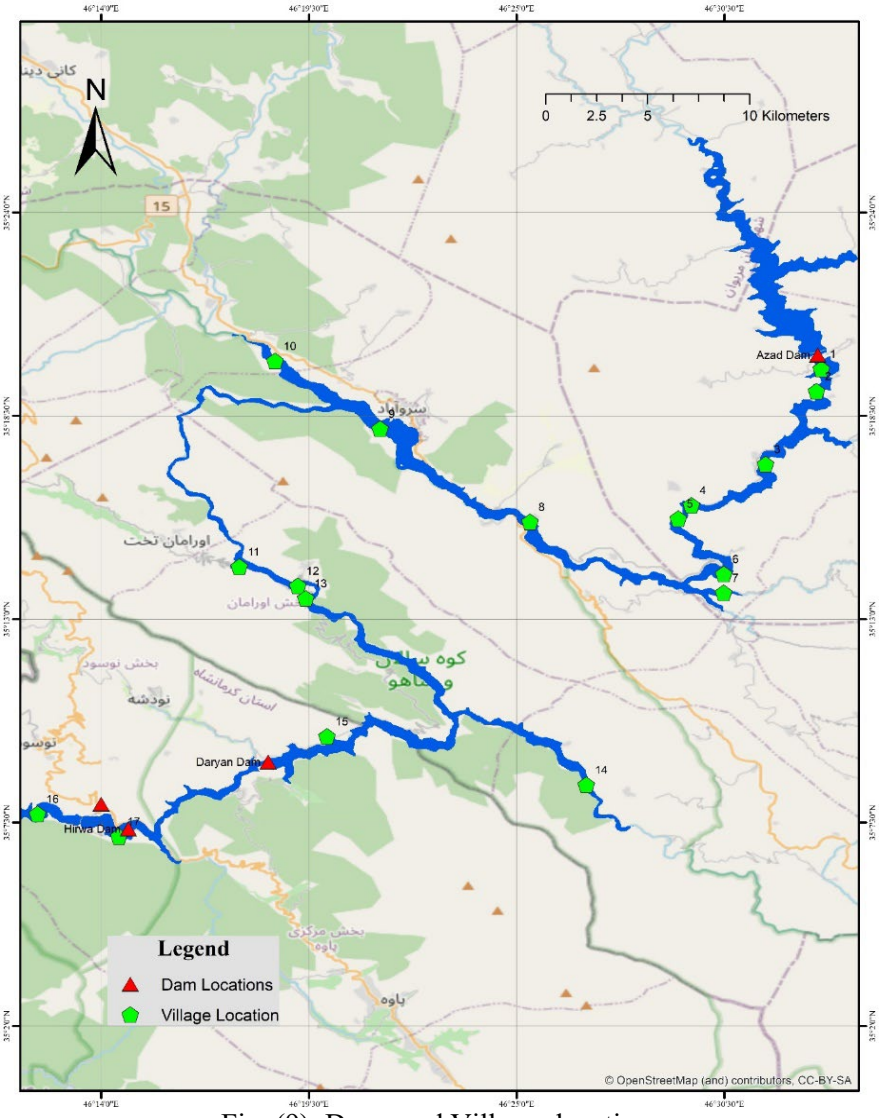

Fig. (9): Dams and Villages location.

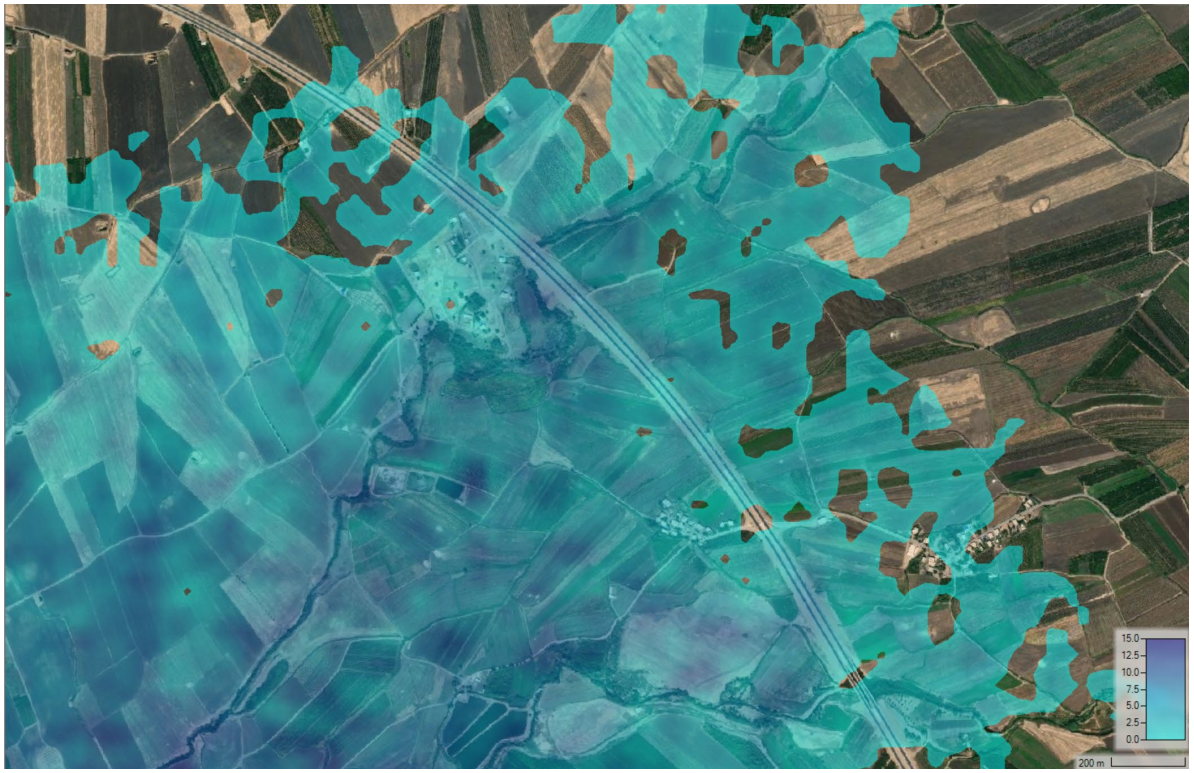

Fig. (10): Halabja new Road approximately over 2m will be submerged.

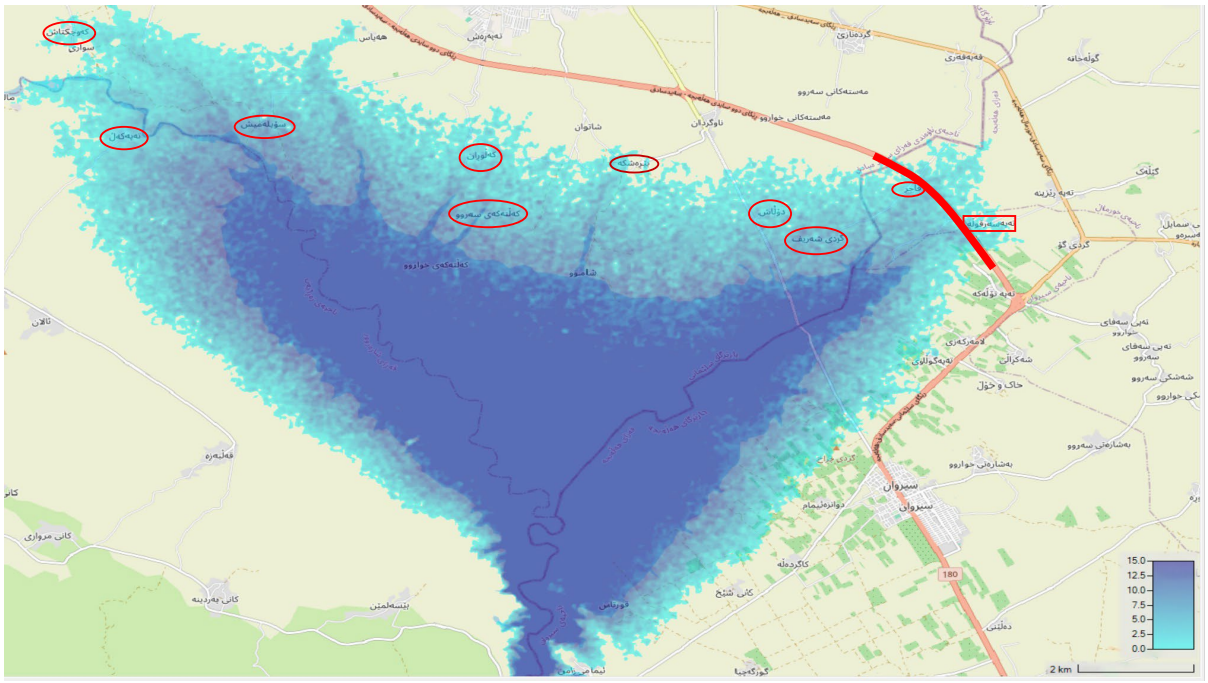

Fig. (11): Iraqi Villages that might be submerged due to upstream dam failures.

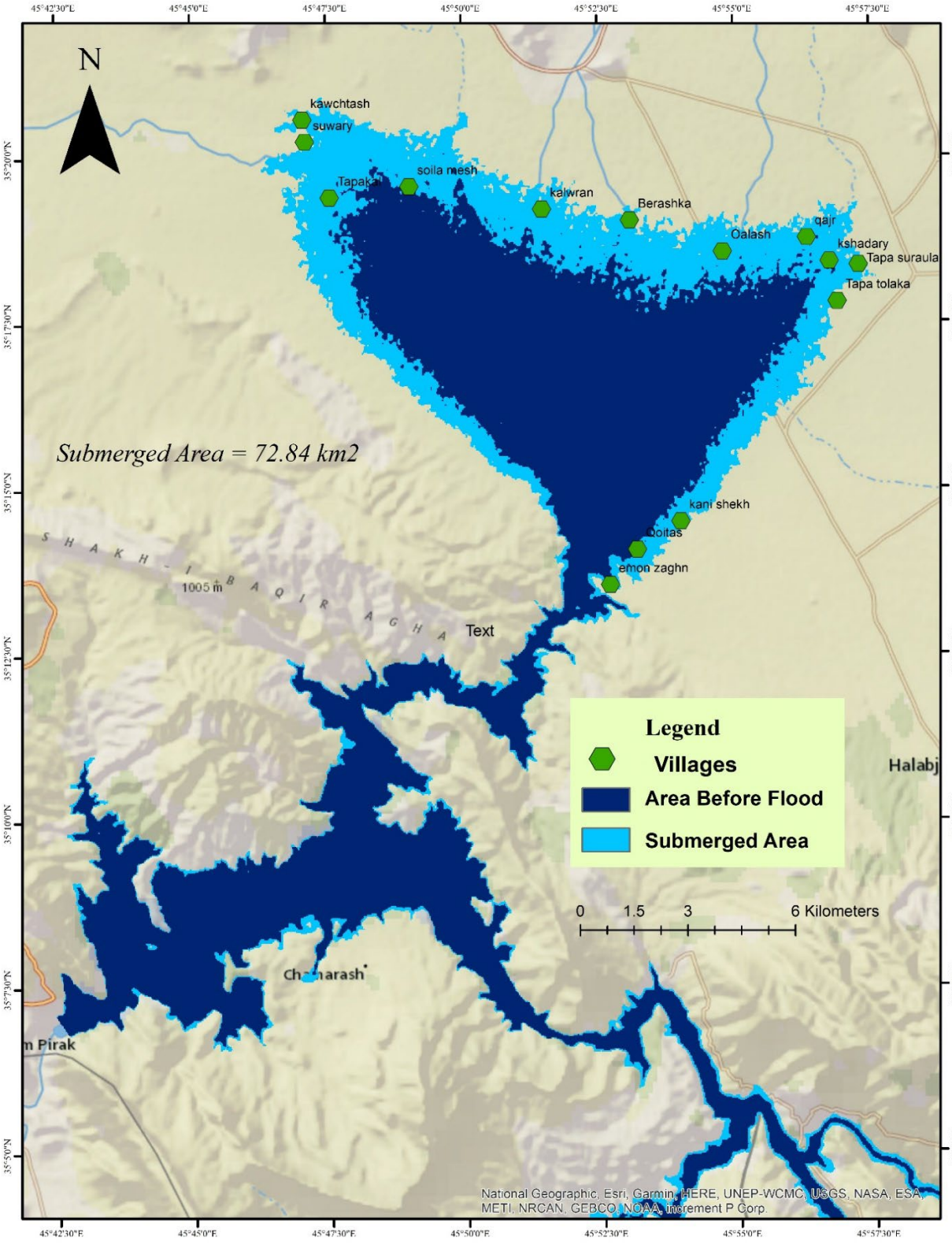

Fig. (12): Submerged Area after flood

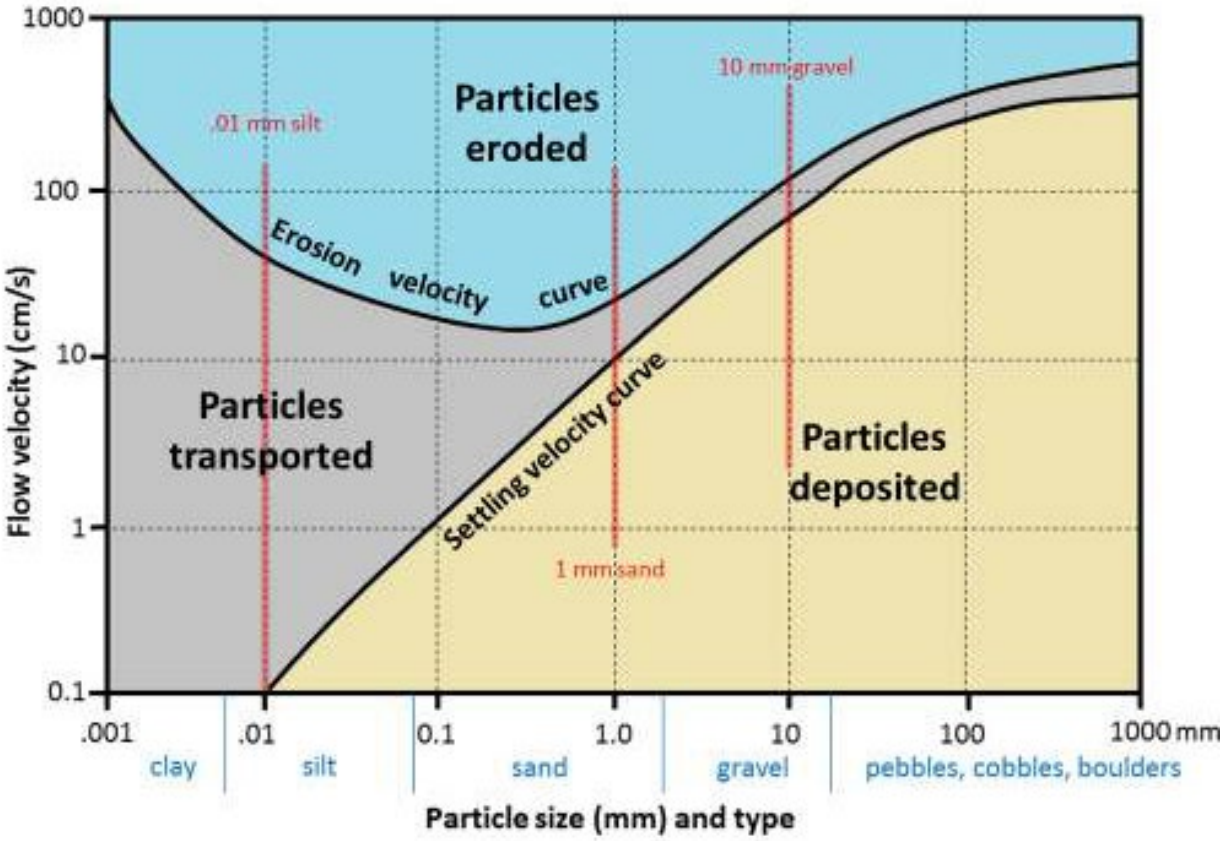

Fig. (13): Hjulström diagram [47]

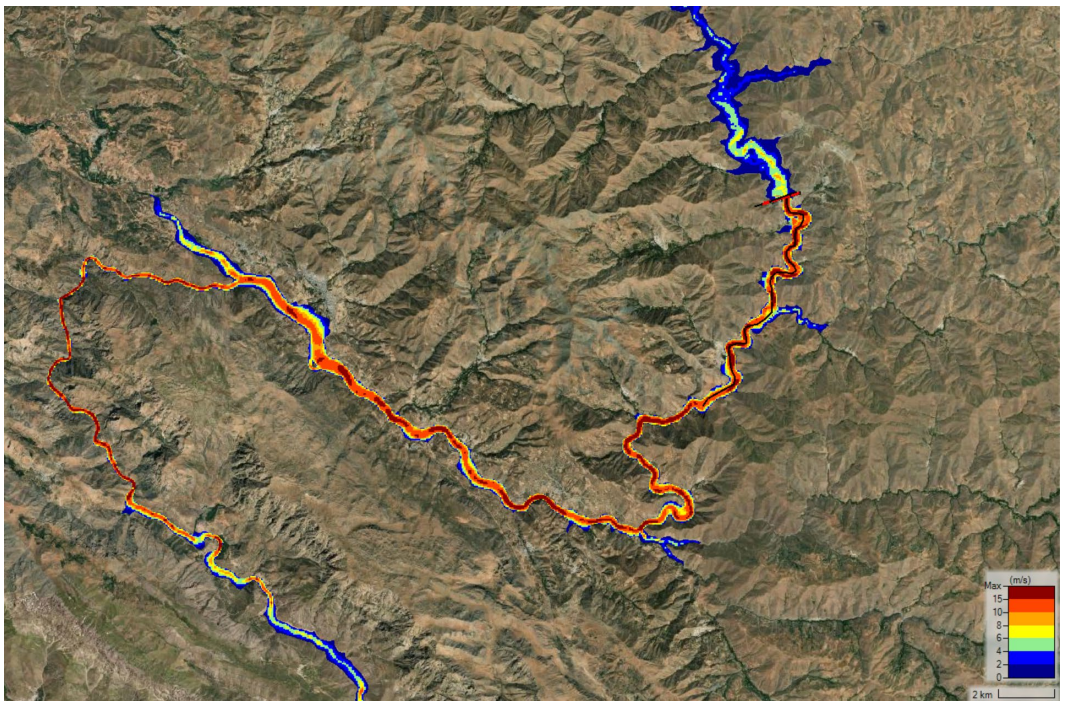

Fig. (14): Flood Velocity from Azad dam to Daryan dam.

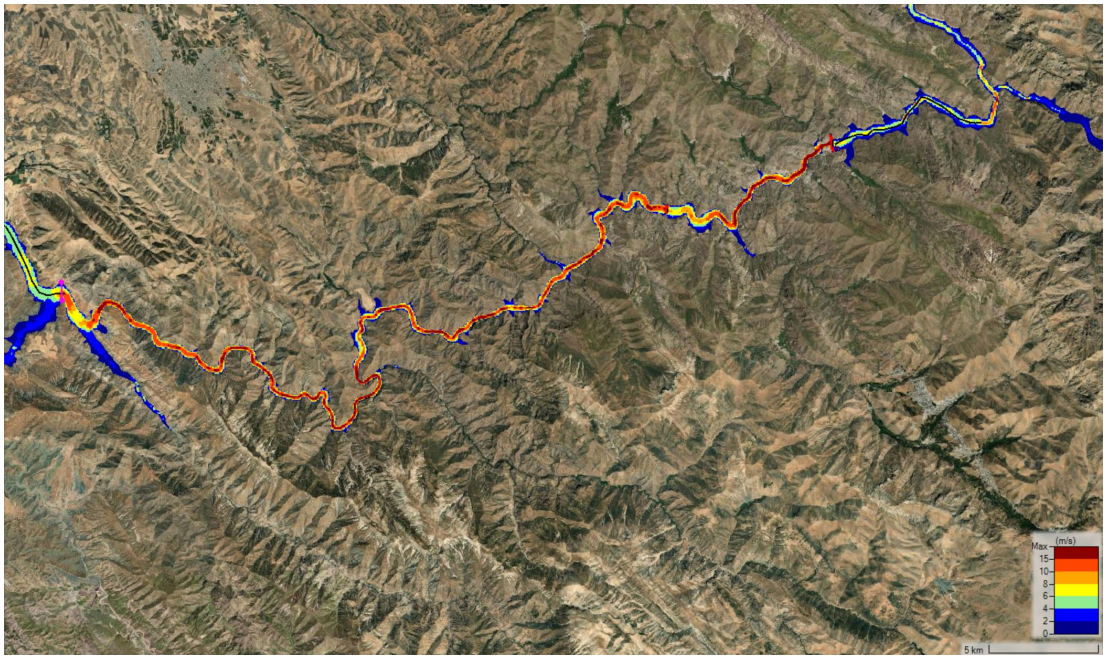

Fig. (15): Flood wave from Daryan dam to Darbandikhan dam.